Cr^{3+} in layered perovskites: do the electron paramagnetic resonance parameters only depend on the impurity–ligand distances?

2010 J. Phys.: Condens. Matter 22 155502

(http://iopscience.iop.org/0953-8984/22/15/155502)

J. Phys.: Condens. Matter **22** (2010) 155502 (7pp) doi:10.1088/0953-8984/22/15/155502

Cr^{3+} in layered perovskites: do the electron paramagnetic resonance parameters only depend on the impurity–ligand distances?

J M García-Lastra[1], M T Barriuso[2], J A Aramburu[3] and M Moreno[3]

[1] Nano-Bio Spectroscopy Group and European Theoretical Spectroscopy Facility (ETSF), Departamento Fisica de Materiales UPV/EHU, Apartado 1072, 20018 San Sebastián, Spain
[2] Departamento de Física Moderna, Universidad de Cantabria, E-39005 Santander, Spain
[3] Departamento de Ciencias de la Tierra y Física de la Materia Condensada, Universidad de Cantabria, E-39005 Santander, Spain

E-mail: scpgalaj@ehu.es

Received 13 December 2009, in final form 13 February 2010
Published 26 March 2010
Online at stacks.iop.org/JPhysCM/22/155502

Abstract

The actual value of axial, R_{ax}, and equatorial, R_{eq}, impurity–ligand distances for Cr^{3+} embedded in tetragonal K_2MgX_4 (X = F, Cl) lattices has been explored by means of density functional theory (DFT) calculations on clusters involving up to 69 ions using two different functionals. For K_2MgF_4:Cr^{3+} R_{eq} and R_{ax} are found to be coincident within only 0.5 pm. When the **g** tensor of K_2MgF_4:Cr^{3+} is derived considering only the CrF_6^{3-} unit *in vacuo* at the calculated equilibrium geometry the $g_\perp - g_\parallel$ quantity fails to reproduce the experimental value by one order of magnitude. In contrast, when the active electrons localized in the CrX_6^{3-} complex (X = F, Cl) are allowed to feel the anisotropic electric field coming from the rest of the lattice ions the splitting in the first excited state, $^4T_2$, increases by one order of magnitude. The present results thus show that the **g** tensor anisotropy and the zero-field splitting constant, D, observed for K_2MgX_4:Cr^{3+} (X = F, Cl) are not mainly due to a local deformation of the CrX_6^{3-} octahedron but to the action of the internal electric field, often ignored when seeking the microscopic origin of electronic properties due to impurities in insulating lattices. Accordingly, serious doubts on the validity of the superposition model are cast by the present work.

(Some figures in this article are in colour only in the electronic version)

1. Introduction

The lack of translational symmetry makes it, in principle, more difficult to understand the properties of a doped material than those of a pure crystalline compound. This serious drawback is, however, greatly overcome in the case of insulating host lattices due to the *localization* of active electrons [1–4]. In particular, when a transition metal impurity, M, is placed in an insulator its valence electrons are usually confined in the MX_N complex formed by the impurity itself and the N nearest anions or ligands [4, 5]. This confinement is experimentally well proved by electron paramagnetic resonance (EPR) [6] and especially electron nuclear double resonance (ENDOR) [7] measurements which provide us with useful information on the electronic density coming from unpaired electrons.

By virtue of these facts it has widely been assumed that an understanding of electronic properties like the gyromagnetic (**g**) tensor or the optical absorption peaks due to a transition metal (TM) impurity *only* requires one to know: (i) the position of the impurity in the host lattice and thus the nature of the MX_N complex formed inside, (ii) the existence of possible defects coupled to the impurity and (iii) the distances

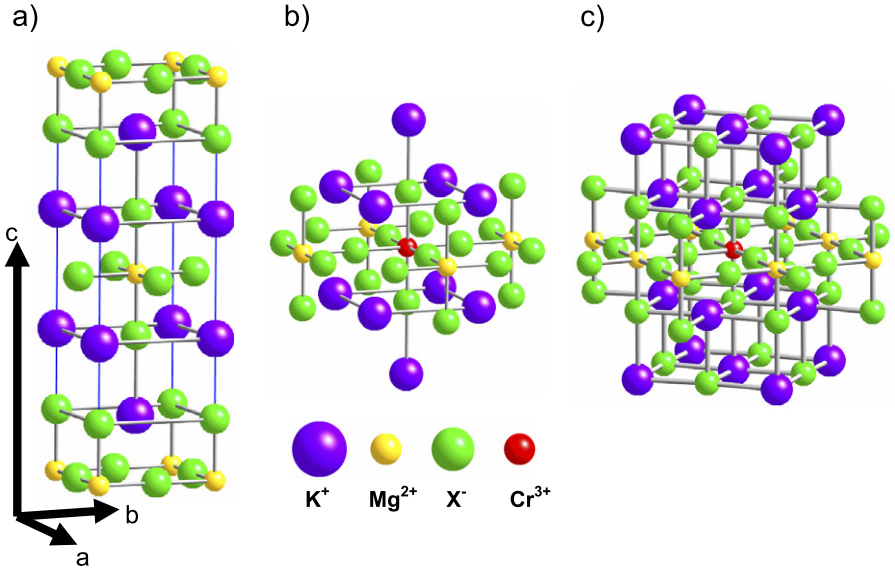

Figure 1. (a) Unit cell of the K_2MgX_4 lattice (X = F, Cl). (b) View of the 37-atom cluster used in the DFT calculations. (c) View of the 69-atom cluster used for checking the convergence of the results of the 37-atom cluster.

between the impurity and all ligands [3–7]. The advent of reliable information on the actual values of the impurity–ligand distances, however, cast doubts on the general validity of the last assumptions [4, 8]. For instance, the different colour displayed by ruby and emerald cannot be explained on the basis of a different mean Cr^{3+}–O^{2-} distance in both systems. Indeed recent EXAFS measurements have proved that they are coincident within 1 pm [9, 10]. Seeking to clarify this situation it has been argued [8, 11–13] that an MX_N unit is never isolated but embedded in an insulating lattice formed by ions. The ions lying *outside* that unit give rise to an internal electric field, **E**, whose influence on the electronic properties of the complex cannot thus be neglected *a priori*. Along this line theoretical calculations considering only the CrO_6^{9-} complex but including the effects of **E** explain rather reasonably the colour shift among the different Cr^{3+}-based gemstones [8, 11]. In accordance with these results it can be expected that EPR parameters associated with a given TM impurity in an insulator can *also* be sensitive to the form of the internal electric field undergone by the complex.

The present work is devoted to gaining a better insight into the experimental **g** tensor due to Cr^{3+} impurities in compounds with the *tetragonal* K_2NiF_4 structure (figure 1(a)), which belongs to the *I*4/*mmm* spatial group (number 139). Different centres are formed in lattices like K_2MgF_4, K_2ZnF_4 [14], K_2MgCl_4 [15] or Rb_2ZnF_4 [16] doped with Cr^{3+} where in all cases the impurity replaces the divalent cation of the host lattice. Some of the centres involve close vacancies to Cr^{3+} leading to an experimental spin-Hamiltonian displaying orthorhombic symmetry. Nevertheless, in all lattices another Cr^{3+} centre is observed whose spin-Hamiltonian exhibits a perfect tetragonal symmetry, and where the principal axis of both the **g** and zero-field splitting tensors is just the crystal **c** axis (figure 1(a)). Moreover, an ENDOR study of the superhyperfine tensors does not provide us with any measurable evidence of a lack of local D_{4h} symmetry around Cr^{3+}. These reasons thus support that the required charge compensation in that the Cr^{3+} centres are far apart [14, 15]. It should be pointed out that under replacement of a host cation, H^{p+}, by an impurity, I^{q+}, with $p \neq q$ powerful techniques like EPR and especially ENDOR have proved the formation of centres with remote charge compensation. This situation is found, for instance, in the so-called cubic centres formed in Cr^{3+}-or Fe^{3+}-doped $KMgF_3$ [17–19] where ENDOR data do not show any deviation from a strict O_h local symmetry. In the same vein the dominant C_{2V} centre formed in NaCl:Rh^{2+} involves a close Na^+ vacancy [7, 20]. However, by thermal treatments the close vacancy can be dissociated from the rhodium impurity, thus leading to a pure Jahn–Teller centre with D_{4h} symmetry [20].

The present study shall be focused on this free-vacancy Cr^{3+} centre formed in layered perovskites like K_2MgF_4. For this centre $g_\parallel = 1.9727$ and $g_\perp = 1.9743$ values have been reported [14]. Close figures have been measured for the same centre in K_2ZnF_4 ($g_\parallel = 1.9733$, $g_\perp = 1.9740$) [14], Rb_2ZnF_4 ($g_\parallel = 1.9722$, $g_\perp = 1.9746$) [16] or Rb_2CdF_4 ($g_\parallel = 1.9710$, $g_\perp = 1.9742$) [16]. In all cases it is found $|g_\parallel - g_0| > |g_\perp - g_0|$. A similar situation is also encountered for the free-vacancy centre in K_2MgCl_4:Cr^{3+}, where $g_\parallel = 1.9831$ and $g_\perp = 1.9846$ [15].

The anisotropy exhibited by the experimental **g** tensor has been interpreted [21–23] *assuming* that in all cases the CrX_6^{3-} complex (X = F, Cl) exhibits a tetragonal compressed geometry where the equilibrium Cr^{3+}–X^- distance along the crystal **c** axis, R_{ax}, is smaller than the equatorial one, R_{eq}. Different authors using parametrized models have pointed out that a value of $R_{eq} - R_{ax}$ in the 3–5 pm range *might* explain the experimental **g** tensor [21, 22]. However, for being confident on the reliability of this explanation it is crucial first to know what the actual R_{ax} and R_{eq} values are. Once such equilibrium distances are reasonably known one should explore whether

the experimental $g_\perp - g_\parallel$ quantity can or cannot be accounted for considering *only* the *isolated* CrX_6^{3-} unit (X = F, Cl).

Seeking to clarify these issues the systems K_2MgF_4:Cr^{3+} and K_2MgCl_4:Cr^{3+} have been looked into by means of density functional theory (DFT) calculations. As there is no experimental information on the Cr^{3+}–X^- (X = F, Cl) distances in these systems *ab initio* calculations can be of great help in order to gain a better insight into this relevant point. Aside from deriving the R_{ax} and R_{eq} values particular attention is paid to determine the splitting, δ, induced on the first excited state, $^4T_2$ as a result of the tetragonal symmetry. This splitting governs the $g_\perp - g_\parallel$ value which is found experimentally to be close to 2×10^{-3} for K_2MgF_4:Cr^{3+}. For clearing out what is the main factor responsible for δ this quantity has first been derived considering only the isolated CrX_6^{3-} unit at the right equilibrium geometry. In a second step δ has been calculated for the CrX_6^{3-} complex subject to the effects of the internal electric field, **E**.

This paper is arranged as follows. A short account of computational details is given in section 2 while a recall of the microscopic interpretation of the **g** tensor for a CrX_6^{3-} (X = F, Cl) complex is shown in section 3. Results on the equilibrium geometry are reported in section 4 together with the calculated values of the splitting δ and the $g_\perp - g_\parallel$ quantity. The relationship of the present conclusions to the electronic properties displayed by other impurities in insulating lattices is discussed in section 5.

2. Computational details

Calculations have been carried out using the Amsterdam density functional (ADF) code [24]. To support the reliability of obtained results two different exchange–correlation functionals have been used: Vosko–Wilk–Nusair [25] in the local density approximation (LDA), and the generalized gradient approximation (GGA) in its Becke–Lee–Yang–Parr (BLYP) form [26, 27]. All the atoms have been described through basis sets of TZP quality (tripe-ζ Slater-type orbitals plus one polarization function) given in the program database and the core electrons were kept frozen (1s–2s for F, 1s–2p for Mg, 1s–3p for K and 1s–3p for Cr).

Most of the calculations were performed for clusters of 37 ions centred at the impurity which keeps the tetragonal symmetry of the host lattice (figure 1(b)). In every calculation the cluster is not free but feels the electric field coming from the rest of the lattice ions outside the cluster. In the present calculations the position of ligands is derived through energy minimization while the rest of the ions in the cluster have been fixed at the positions given by x-ray diffraction data. The method and cluster are thus the same previously employed [28] for exploring the equilibrium geometry of Mn^{2+} and Ni^{2+} impurities in K_2MgF_4. As a test of its reliability this method leads [28] to R_{ax} and R_{eq} values for the pure K_2MgF_4 lattice which differ by less than 1% from the experimental figures $R_{ax}^0 = 2.005$ Å and $R_{eq}^0 = 1.990$ Å. These values underline that the octahedron surrounding Mg^{2+} in K_2MgF_4 is elongated but very slightly. For being sure about the actual R_{ax} and R_{eq} values for K_2MgF_4:Cr^{3+} and K_2MgCl_4:Cr^{3+} calculations on a 69-ion cluster have also been carried out (figure 1(c)). The differences between the optimized distances found in the 69-ion cluster calculation and those reached in the cluster with 37 ions are *less* than 1 pm. Therefore, it can be considered that the 37-ion cluster calculation results are converged with respect to the cluster size.

For K_2MgF_4:Cr^{3+} the active electrons are found to reside essentially in the CrF_6^{3-} complex which is thus reasonably embedded in a 37-ion cluster. To be more specific, we have verified that 99% of the electronic charge associated with an antibonding $\sim xy$ orbital is localized in the complex. Therefore, a quantum calculation including the complex itself and 30 additional ions forming a buffer is expected to provide us with reasonable values of R_{ax} and R_{eq}.

Once the equilibrium axial and equatorial distances are determined particular attention has been paid to calculate the splitting δ for the CrF_6^{3-} unit either *isolated* or under the internal electric field, **E**. It should be noticed that in the latter case **E** arises from close ions in the buffer as well as from further ions of the whole lattice. These further ions are represented by means of a set of 134 point charges with values previously fitted to reproduce the electrostatic potential corresponding to the infinite system, V_0. Since these lattices are very ionic, it is assumed that V_0 corresponds to the potential created by the nominal charges of the ions. This procedure is thus the same previously used in [8, 11, 27], based on the Ewald code [29].

3. Recall on the g tensor for a CrX_6^{3-} unit in tetragonal symmetry

For a CrX_6^{3-} unit under perfect octahedral symmetry the g shift arises from the admixture, via spin–orbit interaction, of the ground state $^4A_2$ with the only $^4T_2$ state, emerging from the d^3 configuration [5, 6, 30]. As the orbital angular momentum operator, **L**, belongs to T_1 only T_2 states are connected with the ground state as a result of spin–orbit coupling. For a CrF_6^{3-} complex with small or moderate covalency, the g shift is well described by [5, 6]

$$g_0 - g = \frac{8}{3}\frac{\xi^*}{\Delta} \tag{1}$$

where $\Delta = 10$ Dq and ξ^* is the effective spin–orbit coefficient which is *reduced* with respect to that for free Cr^{3+} ion, ξ, due to covalency [6]. Let us consider an antibonding orbital of the CrF_6^{3-} complex briefly described by

$$|\phi_i\rangle = N_i|d_i\rangle - \lambda_i|\varphi_L^i\rangle; \quad i = t, e. \tag{2}$$

Here $|d_i\rangle$ means a d-wavefunction while $|\varphi_L^i\rangle$ stands for a linear combination involving valence orbitals of six ligands. The relation between ξ^* and ξ can be approximated by [30]

$$\xi^* = N_e^2 N_t^2 \xi. \tag{3}$$

Although equation (1) is based on second-order perturbation theory such an expression is quite valid for a complex like CrF_6^{3-} because 10 Dq is around 15 000 cm^{-1} while ξ is only equal to 270 cm^{-1} [5, 6, 22].

Table 1. Calculated values (in Å) of the axial and equatorial metal–ligand distances for K_2MgF_4:Cr^{3+} by means of two different functionals in a 37-atom cluster. For comparison purposes R_{ax} and R_{eq} values for Mn^{2+} and Ni^{2+} impurities in K_2MgF_4 are also shown.

Impurity	Cr^{3+}		Mn^{2+}		Ni^{2+}	
Functional	LDA	BLYP	LDA	BLYP	LDA	BLYP
R_{ax}	1.880	1.900	2.082	2.091	2.002	2.047
R_{eq}	1.885	1.900	2.025	2.031	1.981	1.995

Table 2. Values of the K_T, K_1 and K_2 force constants (all in eV $Å^{-2}$ units) calculated for K_2MgF_4:Cr^{3+}. For comparison purposes results previously derived for divalent impurities in the K_2MgF_4 lattice using a 37-atom cluster are also displayed [28].

	Cr^{3+}			Ni^{2+}			Mn^{2+}		
	K_1	K_2	K_T	K_1	K_2	K_T	K_1	K_2	K_T
Axial	16.94	0.67	17.60	7.33	1.30	8.63	4.81	1.37	6.18
Equatorial	16.54	5.68	22.23	8.77	7.80	16.57	8.00	9.27	17.27

When the complex is subject to a tetragonal perturbation it produces in first order a splitting of the $^4T_2$ state, leading to ^4E and $^4B_2$ states whose energies with respect to the ground state are denoted by Δ_1 and Δ_2, respectively. In such a case $g_\parallel$ and $g_\perp$ can be written as [6, 30]

$$g_0 - g_\perp = \frac{8}{3}\frac{\xi^*}{\Delta_1}; \qquad g_0 - g_\parallel = \frac{8}{3}\frac{\xi^*}{\Delta_2}. \tag{4}$$

Calling now $\Delta_1 - \Delta_2 = \delta$, if $\delta \ll 10$ Dq the quantity $g_\perp - g_\parallel$ is essentially given by

$$g_\perp - g_\parallel = \frac{8}{3}\frac{\xi^*\delta}{(10\ \mathrm{Dq})^2}. \tag{5}$$

Therefore, as $\xi^* < \xi$ it can be concluded that

$$g_\perp - g_\parallel < \frac{8}{3}\frac{\xi\delta}{(10\ \mathrm{Dq})^2}. \tag{6}$$

This simple inequality establishes a link between the δ value calculated at the equilibrium geometry and the $g_\perp - g_\parallel$ quantity measured experimentally.

4. Results and discussion

4.1. Equilibrium geometry for $K_2MgF_4Cr^{3+}$ and K_2MgCl_4:Cr^{3+}

The equilibrium axial and equatorial impurity–ligand distances calculated for K_2MgF_4:Cr^{3+} by means of two different functionals are gathered in table 1. For comparison purposes R_{ax} and R_{eq} values previously derived for Mn^{2+} and Ni^{2+} impurities in K_2MgF_4 are also shown in the same table [28]. As expected the $Mg^{2+} \rightarrow Cr^{3+}$ substitution leads to R_{ax} and R_{eq} values smaller than $R^0_{ax} = 2.005$ Å and $R^0_{eq} = 1.990$ Å corresponding to the perfect lattice.

As a salient feature the results shown in table 1 point out that the CrF_6^{3-} complex embedded in the K_2MgF_4 lattice is practically undistorted from the perfect octahedral geometry. In fact, the difference between R_{eq} and R_{ax} is found to be null using the BLYP functional while it amounts only to 0.5 pm with the LDA. Therefore, the calculated $R_{eq} - R_{ax}$ difference in table 1 is found to be certainly smaller than the figure *estimated* in previous works [21, 22]. The result for K_2MgF_4:Cr^{3+} in table 1 is seemingly surprising when compared to the R_{ax} and R_{eq} values found [28] for Mn^{2+} and Ni^{2+} impurities in K_2MgF_4. Let $t = 2(R_{ax} - R_{eq})/(R_{eq} + R_{ax})$ be the tetragonality parameter for CrF_6^{3-} or MF_6^{4-} (M = Mn, Ni) units in K_2MgF_4. According to table 1 while $|t|$ is found to lie around 3% for MnF_6^{4-} it is smaller than 0.3% for CrF_6^{3-}.

The study of the force constants, K_T^{ax} and K_T^{eq}, corresponding to the displacement of an axial and an equatorial ligand ion, respectively, along the metal–ligand direction, sheds light on this remarkable difference. In a simple model, the total force constants K_T^j (j = ax, eq) can thus be considered to involve two contributions [4, 31]:

$$K_T^j = K_1^j + K_2^j \qquad (j = \mathrm{ax}, \mathrm{eq}). \tag{7}$$

Here K_1^j and K_2^j (j = ax, eq) refer to the force constants coming, respectively, from the metal–ligand bond and that involving the ligand and the *next-nearest* neighbour to the central ion for both axial and equatorial ligands. Values of K_T^j, K_1^j and K_2^j (j = ax, eq) force constants derived from the present calculations for K_2MgF_4:Cr^{3+} are gathered in table 2 and compared to previous results reached on Mn^{2+} and Ni^{2+} impurities in the same host lattice [28]. It can be noticed that in all cases $K_2^{eq} \gg K_2^{ax}$. As has previously been emphasized [32], this remarkable anisotropy reflects the layered structure of K_2MgF_4. Indeed, as shown in figure 1, the *next-nearest* neighbour of a Mg^{2+} cation along the **a** or **b** axis is also a divalent cation while it is a monovalent K^+ ion if we move along the principal **c** axis.

It is worth noting now that while for K_2MgF_4:M^{2+} (M = Mn, Ni) K_2^{eq} is found to be comparable to K_1^{eq} this situation is no longer true for K_2MgF_4:Cr^{3+} where the metal–ligand force constant K_1^{eq} is much higher than K_2^{eq}. This fact is thus a manifestation of significant *elastic decoupling* of the CrF_6^{3-} complex from the rest of the K_2MgF_4 lattice, a phenomenon which usually takes place when a host cation is replaced by another one with higher nominal charge [4, 33]. As a result of this elastic decoupling, it turns out that the ratio K_T^{eq}/K_T^{ax} is equal only to 1.25 for K_2MgF_4:Cr^{3+} while a higher value $K_T^{eq}/K_T^{ax} = 2.8$ is reached for K_2MgF_4:Mn^{2+}. As Mn^{2+} has an ionic radius higher than that of Mg^{2+} the significant difference between K_T^{eq} and K_T^{ax} thus explains the existence of elongated equilibrium geometry for K_2MgF_4:Mn^{2+}. In contrast, in the case of K_2MgF_4:Cr^{3+}, the equilibrium geometry is found to be compressed but very slightly. This result is thus in qualitative agreement with K_T^{eq} and K_T^{ax} values of table 2 and an ionic radius of Cr^{3+} a little smaller than that of Mg^{2+}.

A bigger $R_{eq} - R_{ax}$ value is expected for K_2MgCl_4, a softer lattice than K_2MgF_4. Using the LDA functional it is found for K_2MgCl_4 $R_{ax} = 2.305$ Å and $R_{eq} = 2.330$ Å thus implying $R_{eq} - R_{ax} = 2.5$ pm. A $R_{eq} - R_{ax}$ value equal to 3.1 pm is

Table 3. Calculated values (in cm^{-1}) of the splitting in the $^4T_2$ state, δ, for CrX_6^{3-} units in K_2MgX_4 (X = F, Cl) at the equilibrium geometry using LDA. The first line collects the results for the isolated complex while in the second line are shown the δ values obtained once the complex is allowed to feel the internal electric field, **E**, arising from the rest of the lattice ions not involved in the CrX_6^{3-} unit. Equilibrium values are $R_{ax} = 1.880$ Å and $R_{eq} = 1.885$ Å for $K_2MgF_4:Cr^{3+}$ and $R_{ax} = 2.305$ Å and $R_{eq} = 2.330$ Å for $K_2MgCl_4:Cr^{3+}$.

	$K_2MgF_4:Cr^{3+}$	$K_2MgCl_4:Cr^{3+}$
δ (isolated complex)	65	73
δ (with the internal field)	976	1113

obtained by means of the BLYP functional although the values of R_{eq} and R_{ax} are found to be 2.5% higher than using the LDA.

4.2. Calculation of the splitting δ and the g tensor for the isolated complex

Once the equilibrium geometry of CrX_6^{3-} units in K_2MgX_4 (X = F, Cl) has been established it is crucial to determine what is the value of the splitting δ and the $g_\perp - g_\parallel$ value expected for an *isolated* complex at the right equilibrium geometry. For this goal we have only considered the LDA results which give a non-zero $R_{eq} - R_{ax}$ value for K_2MgF_4.

Values of the splitting in the $^4T_2$ state are given in table 3 for both CrX_6^{3-} (X = F, Cl) units *in vacuo*. It can be noticed that for both systems the splitting δ is calculated to be smaller than 100 cm^{-1}. Let us now take as a guide the case of $K_2MgF_4:Cr^{3+}$ for which the 10 Dq is found to be equal to 14 750 cm^{-1}. Using this value together with $\delta = 65$ cm^{-1} the inequality (6) leads to the conclusion that the experimental $g_\perp - g_\parallel$ quantity should be positive and smaller than 2×10^{-4}. This figure is, however, one order of magnitude smaller than the value $g_\perp - g_\parallel = 1.6 \times 10^{-3}$ measured experimentally [14]. Therefore, the small compression of the CrF_6^{3-} unit in K_2MgF_4 derived from the present calculations through the LDA functional can hardly be mainly responsible for the **g**-tensor anisotropy well observed experimentally.

4.3. Effects of the internal electric field on the splitting δ and the g tensor

As has already been pointed out, although active electrons are well localized in the CrX_6^{3-} (X = F, Cl) unit it does not mean that the electronic properties associated with the Cr^{3+} impurity can be explained considering *only* that isolated complex. In fact, the rest of the ions of the K_2MgX_4 (X = F, Cl) host lattice can create an electric field, $\mathbf{E} = -\nabla V_R(\mathbf{r})$, upon the electrons disseminated in the complex region. In figure 2 is portrayed the calculated value of $V_R(\mathbf{r})$ when **r** is along the crystallographic **a** and **c** axes. It can be noticed that, according to symmetry, there is no electric field on the chromium ion but it appears at ligand sites. In particular $(-e)V_R(\mathbf{r})$ becomes higher when **r** is parallel to **c** than when **r** is along **a** or **b** axes. This fact alone already produces a splitting in the antibonding $e_g(\sim 3z^2-r^2; \sim x^2-y^2)$ orbitals. According to the form of $(-e)V_R(\mathbf{r})$ in the ligand region it can

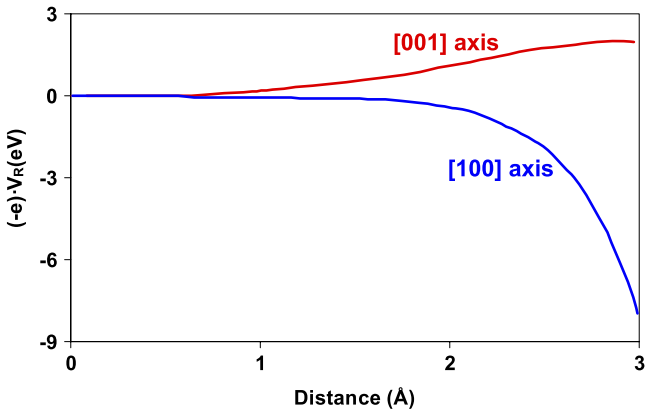

Figure 2. Electrostatic potential, $V_R(\mathbf{r})$, of the rest of the lattice along [1 0 0] and [0 0 1] directions on a seven-atom cluster.

be expected that the molecular orbital $\sim 3z^2-r^2$ has a higher energy than the $\sim x^2-y^2$ one. This means that the splitting in $e_g(\sim 3z^2-r^2; \sim x^2-y^2)$ orbitals produced by the electric field due to the rest of the ions of the K_2MgX_4 lattice on the CrX_6^{3-} (X = F, Cl) complex is qualitatively similar to that expected for an isolated unit under compression along the OZ axis.

The calculated values of the splitting δ for CrX_6^{3-} (X = F, Cl) units under the influence of the internal electric field in the K_2MgX_4 (X = F, Cl) host lattice are also shown in table 3. These values, calculated at the equilibrium geometry, are one order of magnitude bigger than those derived for an isolated complex using the LDA. Furthermore, quite similar values of δ are found for a *perfect* octahedral complex feeling the internal electric field of K_2MgX_4 (X = F, Cl) host lattices. For instance, making $R_{ax} = R_{eq} = 1.883$ Å for CrF_6^{3-} in K_2MgF_4 it is obtained that $\delta = 919$ cm^{-1} while a δ value equal to 1032 cm^{-1} is derived for $CrCl_6^{3-}$ in K_2MgCl_4 assuming $R_{ax} = R_{eq} = 2.32$ Å.

Considering now the $\delta = 976$ cm^{-1} value of table 3 for $K_2MgF_4:Cr^{3+}$ the inequality (6) gives rise to $g_\perp - g_\parallel < 3.2 \times 10^{-3}$ which is thus consistent with experimental findings. Moreover, from the present calculations it is obtained that $N_t^2 = 0.87$, $N_e^2 = 0.78$ and $\Delta_1 = 16\,000$ cm^{-1}. Therefore, taking into account (3) and (4) it is derived for $K_2MgF_4:Cr^{3+}$ $g_\parallel = 1.9723$ and $g_\perp = 1.9740$. These figures are thus not far from the values $g_\parallel = 1.9727$ and $g_\perp = 1.9743$ measured experimentally [14] for $K_2MgF_4:Cr^{3+}$.

Seeking to provide further arguments on the origin of the **g**-tensor anisotropy for $K_2MgF_4:Cr^{3+}$ and $K_2MgCl_4:Cr^{3+}$ we have also calculated what is the required distortion on an *isolated* complex in order to get the δ values collected in table 3. Calculations give $R_{eq} - R_{ax} \approx 20$ pm for both $K_2MgX_4:Cr^{3+}$ (X = F, Cl) systems. This quantity is thus much bigger than the equilibrium $R_{eq} - R_{ax} = 0.5$ and 2.5 pm values derived, respectively, for $K_2MgF_4:Cr^{3+}$ and $K_2MgCl_4:Cr^{3+}$ by means of the LDA.

5. Final remarks

From the present analysis the **g**-tensor anisotropy observed for the free-vacancy Cr^{3+} centre formed in tetragonal layered

perovskites like K_2MgF_4 is not due to the compression of the CrF_6^{3-} octahedron. In contrast, the arguments shown in this work strongly support that the **g**-tensor anisotropy displayed by the free-vacancy Cr^{3+} centre in this kind of lattice is a *direct* reflection of the internal electric field, **E**. The key role played by this internal field for a right interpretation of the $g_\perp - g_\parallel$ quantity measured in K_2MgF_4:Cr^{3+} is founded on two fundamental facts. On the one hand, the calculated R_{eq} and R_{ax} values are essentially coincident as a result of a significant elastic decoupling of the CrF_6^{3-} complex from the rest of the K_2MgF_4 lattice. This fact thus avoids any interpretation of $g_\perp - g_\parallel$ based solely on the compression of the CrF_6^{3-} octahedron. On the other hand, the calculated electric field, **E**, due to all ions lying outside the complex, exhibits a remarkable anisotropy as shown in figure 2 which turns out to be the real cause of the $g_\perp - g_\parallel$ difference.

It should be stressed now that the role played by **E** for understanding the electronic properties of impurities in insulators has often been ignored [34, 35]. Nevertheless, the different colour exhibited by ruby and emerald [4, 8] has been shown to reflect the different shape of the internal field in two lattices which are not isomorphous. The same cause has been demonstrated to be responsible [36, 37] for the distinct properties due to M^{2+} impurities (M = Mn and Ni) in normal and inverted perovskite lattices [38–40].

According to the present results a correct understanding of $g_\perp - g_\parallel$ for transition metal impurities in insulators with a local tetragonal symmetry requires us to consider the influence of the internal electric field on the complex and not only its local deformation. The influence of this field upon the **g**-tensor anisotropy can thus be of importance in cases such as K_2ZnF_4:Cu^{2+} [41], K_2MgF_4:Ni^+ [42] and also in the $CuL_4NH_3^{2-}$ centre formed in NH_4L:Cu^{2+} (L = Cl, Br) where Cu^{2+} occupies an interstitial position and has a local D_{4h} symmetry [43]. Along this line it has been shown [13] that the internal electric field, **E**, plays a key role for explaining the charge transfer spectra observed for NH_4L:Cu^{2+} (L = Cl, Br) [44].

Obviously the internal electric field, **E**, can also play a relevant role in a right interpretation of other spin-Hamiltonian parameters. In particular, in the spin Hamiltonian of a Kramers ion with $S > 1/2$ under tetragonal symmetry appears the zero-field splitting term described by $H_{ZFS} = D\,(S_Z^2 - S^2/3)$, where the D parameter is somewhat related to the **g**-tensor anisotropy. If we only consider the excited states coming from the $^4T_2$ state D can be approximated by $(g_\parallel - g_\perp)\xi^*/6$. This expression leads to $D < 0$ in qualitative agreement with the value $D = -1130$ MHz measured experimentally for K_2MgF_4:Cr^{3+} [14]. It should be noted, however, that at variance with what happens for the **g** tensor the excited states with $S = 1/2$ also play a role for explaining the experimental D value of Cr^{3+} impurities. Despite this fact the results of this work support that D for Cr^{3+} K_2MgF_4:Cr^{3+} is the result of the internal electric field undergone by the CrF_6^{3-} complex. The use of monovalent ions, such as Fe^+, with 10 Dq values lower than that for Cr^{3+} in a layered lattice, might give rise to an increase of the D value [45].

The present results also show that the superposition model [46], widely used [21, 22, 47–49] in the interpretation of EPR and optical data of TM impurities, is not correct. In fact, according to such a model EPR parameters like $g_\parallel$, $g_\perp$ or D are assumed to depend only on R_{ax} and R_{eq}, a statement which is against the present conclusions. Failures of the superposition model have also been demonstrated [4, 50] in the analysis of axial and equatorial superhyperfine tensors for the $FeOF_5^{4-}$ centre formed in $KMgF_3$ [4, 49] and also for the MnF_6^{4-} unit formed in K_2MgF_4 [28].

As a main conclusion, even if active electrons coming from a TM impurity, are highly localized in an MX_N complex, an insight into its electronic properties requires taking into account the internal electric field created on the complex region by the rest of the lattice ions.

It is worth noting that a previous study carried out on d^9 ions in layered perovskites has demonstrated the key role played by the internal electric field for understanding both the equilibrium geometry and the electronic structure. Both features follow a pattern markedly different from that observed for Jahn–Teller ions embedded in *perfect cubic* host lattices [32, 51]. Further work on the influence of the internal electric field on the properties of impurities and mixed crystal is underway.

Acknowledgment

The support by the Spanish Ministerio de Ciencia y Tecnología under FIS2009-07083 is acknowledged.

References

[1] Resta R 2002 *J. Phys.: Condens. Matter* **14** R625
[2] Kohn W 1968 *Many Body Physics* (New York: Gordon and Breach)
[3] Spaeth J M, Niklas J R and Bartram R H 1992 *Structural Analysis of Point Defects in Solids* (Berlin: Springer)
[4] Moreno M, Barriuso M T, Aramburu J A, Garcia-Fernandez P and Garcia-Lastra J M 2006 *J. Phys.: Condens. Matter* **18** R315
[5] Sugano S, Tanabe Y and Kamimura H 1970 *Multiplets of Transition-Metal Ions in Crystals* (New York: Academic)
[6] Abragam A and Bleaney B 1970 *Electron Paramagnetic Resonance of Transition Ions* (Oxford: Clarendon)
[7] Spaeth J M and Koschnick F K 1991 *J. Phys. Chem. Solids* **52** 1
[8] Garcia-Lastra J M, Barriuso M T, Aramburu J A and Moreno M 2005 *Phys. Rev.* B **72** 113104
[9] Gaudry E, Cabaret D, Brouder C, Letard I, Rogalev A, Wilhlem F, Jaouen N and Sainctavit P 2007 *Phys. Rev.* B **76** 094110
[10] Gaudry E, Kiratisin A, Sainctavit P, Brouder C, Mauri F, Ramos A, Rogalev A and Goulon J 2003 *Phys. Rev.* B **67** 094108
[11] Garcia-Lastra J M, Aramburu J A, Barriuso M T and Moreno M 2006 *Phys. Rev.* B **74** 115118
[12] Pierloot K, Van Praet E and Vanquickenborne L G 1992 *J. Chem. Phys.* **96** 4163
[13] Aramburu J A and Moreno M 1997 *Phys. Rev.* B **56** 604
[14] Takeuchi H, Arakawa M, Aoki H, Yosida T and Horai K 1982 *J. Phys. Soc. Japan* **51** 3166
[15] Takeuchi H, Tanaka H, Mori M, Ebisu H and Arakawa M 2002 *Epr in the 21st Century: Basics and Applications to Material, Life and Earth Sciences* (Amsterdam: Elsevier) p 213

[16] Arakawa M, Ebisu H and Takeuchi H 1986 *J. Phys. Soc. Japan* **55** 2853
[17] Davies J J and Horai K 1971 *J. Phys. C: Solid State Phys.* **4** 682
[18] Duvarney R C, Niklas J R and Spaeth J M 1981 *Phys. Status Solidi* b **103** 329
[19] Mortier M, Wang Q, Buzare J Y, Rousseau M and Piriou B 1997 *Phys. Rev.* B **56** 3022
[20] Vercammen H, Schoemaker D, Briat B, Ramaz F and Callens F 1999 *Phys. Rev.* B **59** 11286
[21] Du M L and Zhao M G 1990 *Solid State Commun.* **76** 565
[22] Chai R P, Kuang X Y, Duan M L, Zhang C X and Guo H L 2008 *Mol. Phys.* **106** 999
[23] Takeuchi H and Arakawa M 1994 *J. Phys.: Condens. Matter* **6** 3253
[24] Velde G T, Bickelhaupt F M, Baerends E J, Guerra C F, Van Gisbergen S J A, Snijders J G and Ziegler T 2001 *J. Comput. Chem.* **22** 931
[25] Vosko S H, Wilk L and Nusair M 1980 *Can. J. Phys.* **58** 1200
[26] Becke A D 1988 *Phys. Rev.* A **38** 3098
[27] Lee C T, Yang W T and Parr R G 1988 *Phys. Rev.* B **37** 785
[28] Garcia-Lastra J M, Barriuso M T, Aramburu J A and Moreno M 2009 *Chem. Phys. Lett.* **473** 88
[29] Piken A G and Van Gool W 1968 *Ewald Program* (version modified by J A Aramburu)
[30] Lacroix R and Emch G 1962 *Helv. Phys. Acta* **35** 592
[31] Garcia-Lastra J M, Wesolowski T, Barriuso M T, Aramburu J A and Moreno M 2006 *J. Phys.: Condens. Matter* **18** 1519
[32] Garcia-Lastra J M, Aramburu J A, Barriuso M T and Moreno M 2004 *Phys. Rev. Lett.* **93** 226402
[33] Garcia-Fernandez P, Sousa C, Aramburu J A, Barriuso M T and Moreno M 2005 *Phys. Rev.* B **72** 155107
[34] Orgel L E 1957 *Nature* **179** 1348
[35] Nassau K 1998 *Color for Science* (Amsterdam: Elsevier)
[36] Garcia-Lastra J M, Buzare J Y, Barriuso M T, Aramburu J A and Moreno M 2007 *Phys. Rev.* B **75** 155101
[37] Trueba A, Garcia-Lastra J M, Barriuso M T, Aramburu J A and Moreno M 2008 *Phys. Rev.* B **78** 075108
[38] Mortier M, Piriou B, Buzare J Y, Rousseau M and Gesland J Y 2003 *Phys. Rev.* B **67** 115126
[39] Henke B, Secu M, Rogulis U, Schweizer S and Spaeth J M 2005 *Phys. Status Solidi* c **2** 380
[40] Rodriguez F, Moreno M, Tressaud A and Chaminade J P 1987 *Cryst. Latt. Defects Amorph. Mater.* **16** 221
[41] Riley M J, Hitchman M A and Reinen D 1986 *Chem. Phys.* **102** 11
[42] Alcala R, Zorita E and Alonso P J 1988 *J. Phys. C: Solid State Phys.* **21** 461
[43] Riley M J, Hitchman M A, Reinen D and Steffen G 1988 *Inorg. Chem.* **27** 1924
[44] Breñosa A G, Moreno M, Rodriguez F and Couzi M 1991 *Phys. Rev.* B **44** 9859
[45] Garcia-Fernandez P, Senn F, Daul C A, Aramburu J A, Barriuso M T and Moreno M 2009 *Phys. Chem. Chem. Phys.* **11** 7545
[46] Newman D J and Ng B 1989 *Rep. Prog. Phys.* **52** 699
[47] Murrieta H, Rubio J and Aguilar G 1979 *Phys. Rev.* B **19** 5516
[48] Zheng W C 1995 *Solid State Commun.* **94** 317
[49] Gnutek P, Yang Z Y and Rudowicz C 2009 *J. Phys.: Condens. Matter* **21** 455402
[50] Aramburu J A, Garcia-Lastra J M, Barriuso M T and Moreno M 2003 *Int. J. Quantum Chem.* **91** 197
[51] Garcia-Lastra J M, Aramburu J A, Barriuso M T and Moreno M 2004 *Chem. Phys. Lett.* **385** 286